Journal of Asian Architecture and Building Engineering

ISSN: 1346-7581 (Print) 1347-2852 (Online) Journal homepage: www.tandfonline.com/journals/tabe20

A new practical model to calculate the reduced compressive strength of pre-damaged lightweight concrete subjected to freezing-thawing cycles

Madi Kargin, Lukpanov Rauan, Jumat Kargin, Sudharshan N. Raman, Thanongsak Imjai, Reyes Garcia & Irwanda Laory

To cite this article: Madi Kargin, Lukpanov Rauan, Jumat Kargin, Sudharshan N. Raman, Thanongsak Imjai, Reyes Garcia & Irwanda Laory (07 Mar 2025): A new practical model to calculate the reduced compressive strength of pre-damaged lightweight concrete subjected to freezing-thawing cycles, Journal of Asian Architecture and Building Engineering, DOI: 10.1080/13467581.2025.2472731

To link to this article: https://doi.org/10.1080/13467581.2025.2472731

© 2025 The Author(s). Published by Informa UK Limited, trading as Taylor & Francis Group on behalf of the Architectural Institute of Japan, Architectural Institute of Korea and Architectural Society of China.

Published online: 07 Mar 2025.

Submit your article to this journal

Article views: 391

View related articles

View Crossmark data

Full Terms & Conditions of access and use can be found at
https://www.tandfonline.com/action/journalInformation?journalCode=tabe20

JOURNAL OF ASIAN ARCHITECTURE AND BUILDING ENGINEERING
https://doi.org/10.1080/13467581.2025.2472731

Taylor & Francis
Taylor & Francis Group

BUILDING STRUCTURES AND MATERIALS

OPEN ACCESS Check for updates

A new practical model to calculate the reduced compressive strength of pre-damaged lightweight concrete subjected to freezing-thawing cycles

Madi Kargin[a], Lukpanov Rauan[b], Jumat Kargin[b], Sudharshan N. Raman[c], Thanongsak Imjai[d], Reyes Garcia[a] and Irwanda Laory[a]

[a]Civil Engineering Stream, School of Engineering, The University of Warwick, Coventry, UK; [b]Technical Physics Department, Eurasian National University, Nur-Sultan, Kazakhstan; [c]Department of Civil Engineering, School of Engineering, Monash University Malaysia, Jalan Lagoon Selatan, Bandar Sunway, Selangor, Malaysia; [d]School of Engineering and Technology, Walailak University, Nakhon Si Thammarat, Thailand

ABSTRACT

Many existing lightweight concrete (LWC) buildings have reached the end of their service life across Eastern Europe and Central Asia. This is manifested as progressive damage in the LWC, which in turn is reflected in a reduced compressive strength (RCS) and in several building collapses. To assess the structural condition of such vulnerable buildings, an accurate estimation of the RCS is necessary. However, limited research exists on the progressive damage and RCS of LWC. This article aims to investigate experimentally and analytically the influence of progressive damage on the compressive strength and thermal properties of LWC. The study also proposes a new thermal-based model to predict the RCS of damaged LWC subjected to freezing and thawing (FnT) cycles. To achieve this, 108 concrete cubes (size 100 mm) were subjected to different pre-damage levels (DL = 0%, 40%, 60%, 75%, 85%, 95%) and to subsequent FnT cycles (30, 60, 90, 120, 150, 180). After this, the thermal conductivity (TC) of the LWC cubes was determined using an innovative ad-hoc test rig. The cubes were finally tested in compression until failure to determine their RCS. The experimental results indicate that the relationship between the TC and RCS follows an approximate linear trend regardless of the number of applied FnT cycles. The TC of the tested cubes consistently reduced as the level of pre-damage and number of FnT cycles increased. At 30 FnT cycles, the TC of severely damaged cubes with DL = 95% (0.518 W/mK) was 58% lower than that of cubes with DL = 0% (0.891 W/mK). Based on the experimental results, a new and practical thermal-based RCS prediction model was derived for damaged LWC, adopting a modified version of Maxwell's equation for homogeneous materials. The experimental results are used to calibrate the new model, which calculates the RCS of LWC based on measured TC values. The proposed model accurately predicts the RCS of LWC cubes, with a Test/Prediction ratio of 1.0 and a Std.Dev. = 0.15. The accuracy of the proposed model is evaluated against LWC cored cylinders from a building located in Karaganda (Kazakhstan), and the model is proven to predict well the RCS of the cored cylinders with a mean T/P ratio of 1.13 (Std.Dev. = 0.26). The findings of this study contribute towards the development of more accurate models to assess progressive damage in LWC and the structural condition of existing buildings exposed to harsh continental climates.

ARTICLE HISTORY
Received 7 November 2024
Accepted 23 February 2025

KEYWORDS
Lightweight concrete; damage; thermal conductivity; freezing-thawing cycles; reduced compressive strength

1. Introduction

Precast lightweight concrete (LWC) panels with light burned clay as a coarse aggregate were extensively used in building construction in the 20th century. Currently, approximately 70 million of such buildings exist throughout Eastern Europe and Central Asia (Hrabovszky-Horváth and Szalay 2014), many of which are 70+ years old and therefore reaching the end of their service life. In Kazakhstan, approximately 29,000 buildings with LWC wall panels exist across the country (Statistics, 2020). Compared to normal-weight concrete, LWC has shown to have better insulation properties (up to 60% higher heat loss resistivity) and good fire resistance (up to 4 h of fire rating) (Cao et al. 2021; Othuman and Wang 2011; Real et al. 2016). However, the harsh continental climate of Kazakhstan and continuous freezing and thawing (FnT) cycles have led to damage in the LWC panels of numerous buildings, thus contributing to structural collapses and human fatalities across the region (Sharikov 2017). FnT combined with damage due to overloading also contribute to concrete damage (Figure 1(a)) and cracking in/around precast LWC panels, which reflects on heat leakage through cracks that are only visible through an infrared spectrum (see Figure 1(b)). Determining the compressive strength of LWC panels exposed to FnT cycles is

CONTACT Reyes Garcia reyes.garcia@warwick.ac.uk Civil Engineering Stream, School of Engineering, The University of Warwick, Library Road, Coventry CV4 7AL, UK

© 2025 The Author(s). Published by Informa UK Limited, trading as Taylor & Francis Group on behalf of the Architectural Institute of Japan, Architectural Institute of Korea and Architectural Society of China.
This is an Open Access article distributed under the terms of the Creative Commons Attribution License (http://creativecommons.org/licenses/by/4.0/), which permits unrestricted use, distribution, and reproduction in any medium, provided the original work is properly cited. The terms on which this article has been published allow the posting of the Accepted Manuscript in a repository by the author(s) or with their consent.

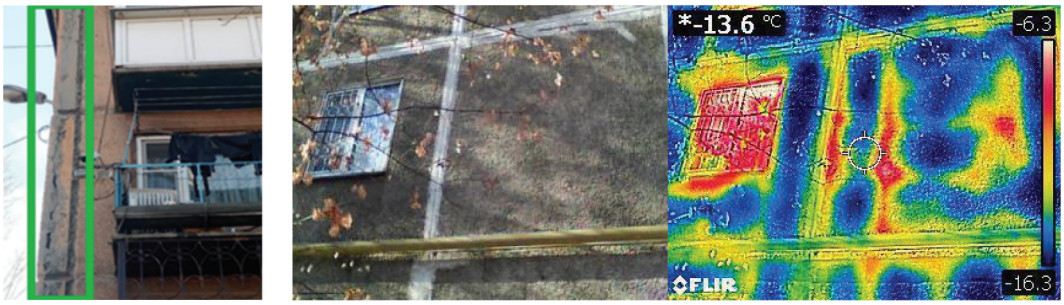

(a) (b)

Figure 1. Damage in LWC buildings (a) spalling around LWC wall panels, (b) local heat leakage through cracks/gaps with visible (L) and infrared spectra (R).

a first necessary step to assess the structural condition of these vulnerable buildings so that cost-effective retrofitting solutions can be implemented to avoid future collapses and loss of life.

Overall, damage in concrete due to the combined effects of FnT cycles and loading is a complex phenomenon that involves a combination of mechanical, physical and chemical processes that are difficult to study individually (Bao et al. 2021; Huang et al. 2019; Karagöl et al. 2018). To bypass this complexity, past research (e.g. Colombo, Colombo, and Di Prisco 2015; Perkowski 2008; Shen et al. 2017) has adopted a "reduced" compressive strength (RCS) and/or the thermal conductivity (TC) of concrete as key parameters to represent damage in a practical way. In particular, FnT cycles have a significant effect on the properties of concrete by causing internal stresses and microstructural damage. This is mainly due to the expansion of water within the concrete pores during freezing (Kosior-Kazberuk 2013), which in turn creates tensile stresses that can exceed the material's tensile strength. Repeated exposure to these cycles results in the formation of microcracks and in the gradual deterioration of the concrete matrix, which can lead to spalling.

Past studies have experimentally investigated the RCS of concrete subjected to FnT cycles, most of them adopting 100 mm cubes. For instance, Yang et al. (2019) found that the RCS of normal concrete reduced by 57% over its maximum compressive strength after 75 FnT cycles. Similarly, Gao et al. (2020), Cao et al. (2021) and Shang and Song (2006) reported that, after 100 FnT cycles, the RCS of normal concrete reduced by 57%, 44% and 54% over the corresponding maximum compressive strengths of intact concrete. Likewise, Wang, Zhou, and Yu Shen (2023) tested cubes of size 250 mm and found that the compressive strength of normal concrete dropped by 52% after 100 FnT cycles (Zhang, Zhou, and Yin 2021). Woo et al. (2021) showed that normal concrete lost 58% and 60% of its maximum compressive strength after 200 and 300 FnT cycles, respectively.

Since the RCS of concrete depends heavily on the mix design and corresponding constituent materials (Sáez Del Bosque et al. 2020), past research has also investigated FnT effects of different types of concretes. For example, Ma, Zhao, and Yang (2017) experimentally investigated the deterioration of compressive strength in normal and air-entrained concrete. The results showed that whilst the compressive strength of normal concrete dropped by 55% after 100 FnT cycles, the strength of air-entrained concrete only dropped by 34% for the same number of cycles. Shang and co-workers (Shang and Song 2006; Shang, Song, and Ou 2009) also showed that air-entrained concrete reduced its strength (by up to 7%) after 100 FnT cycles. The lower drop in compressive strength in air-entrained concrete can be attributed to the presence of voids (internal pores) that can absorb the internal pore pressure of expanded frozen water in the pores, thus allowing air-entrained concrete to withstand FnT cycles much better than normal concrete. Pan et al. (2017) found that the compressive strength of recycled coarse aggregate concrete cubes decreased by up to 57% after 250 FnT cycles. Besides cubes, other types of specimens have been adopted to experimentally study FnT effects on concrete. For instance, Liu et al. (2023) showed that the compressive strength of concrete prisms ($100 \times 100 \times 400$ mm) dropped by up to 45% after to 100FnT cycles. Wardeh, Mohamed, and Ghorbel (2011) found that the compressive strength of concrete cylinders (160×320 mm) reduced by up to 57% after 240 FnT cycles. In general, results from previous research suggest that whilst the compressive strength of concrete consistently reduces with the number of FnT cycles, the type of concrete and aggregate used in the mix can significantly affect the results. Overall, the use of cubic samples in the study of RCS is deemed as a suitable and cost-effective alternative. However, to date, limited research has examined the effect of FnT cycles on LWC samples.

Thermal conductivity (TC) (i.e. the ability to transfer heat) is often used to assess the thermal insulation properties of concrete (e.g. Bindiganavile, Batool, and Suresh 2012; Misri et al. 2018). Moreover, TC has been used to examine changes in concrete subjected to

a certain level of damage, which is usually expressed as a percentage of the maximum concrete compressive strength. For example, Delpak, Gailius, and Žukauskas 2002 experimentally investigated the change of TC in pre-damaged normal concrete cylinders (⌀100 × 200 mm) subjected to a fraction of their maximum compressive strength (0%, 35%, 50% and 75%). It was found that the TC dropped by up to 10% after subjecting the specimens to a pre-damaged level of 75%. Perkowski (2008) investigated the influence of pre-damage on the TC of normal concrete. The TC change measurements were obtained from 40 × 40 × 36 mm cubes, but the compressive strength was obtained from 100 mm cubes. Perkowski reported that the TC dropped by 20% at a pre-damaged level of 95%. More recently, Zhang tested 200 × 200 × 400 mm prisms at pre-damaged levels of 0%, 25%, 40%, 55% and 70%. It was found that the TC dropped by up to 23% at a pre-damaged level of 70%. Models to predict the TC of pre-damaged normal concrete have been also proposed (e.g. Bamforth et al. 2008; Talebi et al. 2020). However, as it will be shown in this study, such models cannot accurately predict the TC of LWC. Based on the above-mentioned observations, it is evident that there is a strong correlation between damage, RCS and TC of concrete. However, to the best authors' knowledge, limited research has examined the TC and RCS of LWC subjected to the combined effect of FnT and pre-damaged. Such model could be useful to assess damage in LWC wall panels of existing buildings, which in turn can be utilised to prevent structural collapses.

Previous research has adopted either general multi-phased theoretical models (e.g. Lu et al. 2021; Maxwell 1873; J. Wang et al. 2006) or semi-empirical models (e.g. Asadi et al. 2018; Antunes Almeida da Silva 2015; Kaur et al. 2023, 2014; Xu et al. 2016; ESCSI 2007) to predict the TC of concrete. However, most of these models can only predict the TC of undamaged normal and LWC (Campbell-Allen et al. 1964; Choktaweekarn, Saengsoy, and Tangtermsirikul 2009; Alengaram et al. 2013), whereas only a few models exist to predict the TC of pre-damaged concrete. One of such models was proposed by Delpak, Gailius, and Žukauskas (2002), who studied the thermal properties of normal concrete cubes subjected to four pre-damaged levels (DL = 0%, 35%, 50%, 75%). However, such model requires the age and moisture contents of the concrete specimen as inputs, which are difficult to know in advance in existing structures. Perkowski (2008) also proposed a TC prediction model for damaged normal concrete. Perkowski assessed the change of heat flux over time on cubes with DL = 0% and DL = 99%. However, Perkowski's model was obtained only for these two DLs and therefore its applicability is somehow limited. More recently, Zhang et al. (2015) proposed two mesoscale TC prediction models for undamaged and pre-damaged (DL = 25%, 40%, 55%, and 70%) normal concrete by extending Maxwell's approach. In Zhang et al.'s model, damage was considered by degrading the modulus of elasticity of concrete as the level of pre-damage increases. However, the model cannot be applied to LWC. The state-of-the-art indicates a lack of experimental and analytical on the RCS and TC of damaged LWC subjected to FnT cycles. Moreover, practical equations to calculate the RCS of LWC subjected to FnT cycles do not exist, and these are necessary to assess more accurately the structural condition of existing LWC buildings exposed to the harsh environmental conditions of Central Asia. Further research is therefore necessary to fill in these gaps in current knowledge.

This article aims to i) investigate experimentally and analytically the influence of damage on the RCS and TC of LWC and ii) propose a new practical model to calculate the RCS of pre-damaged LWC subjected to FnT cycles. For this purpose, 108 concrete cubes (size 100 mm) were subjected to different pre-damaged levels (0%, 40%, 60%, 75%, 85% or 95%) and various FnT cycles (30, 60, 90, 120, 150 or 180 cycles). The experimental results are discussed in terms of the relationships between pre-damaged levels, TC and RCS. Based on the experimental results, the new model is calibrated and subsequently evaluated against test results from cylinder samples cored from actual LWC wall panels of an existing building located in Kazakhstan. The new model is expected to be integrated into a novel framework recently proposed by the authors (Kargin et al. 2022) that can assess damage of existing LWC buildings using satellite infrared images and AI. The findings of this work contribute towards the development of more accurate models to assess progressive damage in LWC buildings exposed to harsh continental climates.

2. Experimental programme

Figure 2 shows a flowchart with the different steps of the experimental programme. The different steps are described in the following sections.

2.1. Cube samples and LWC mix design

A total of 114 cubes (Figure 3) of size 100 mm were cut off (with a circular diamond blade) from a precast LWC wall panel built in the laboratory of the Eurasian National University, Kazakhstan. The wall was cast horizontally to replicate typical practices adopted in the construction of precast walls in the 1950s. The LWC used to cast the wall was produced using locally sourced materials and according to the following mix design (per 1 m^3): Ordinary Portland Cement type CEM II (32.5N) = 450 kg, quarry sand (0–4 mm) = 350 kg, expanded clay aggregate (5–25 mm) = 800 kg, water

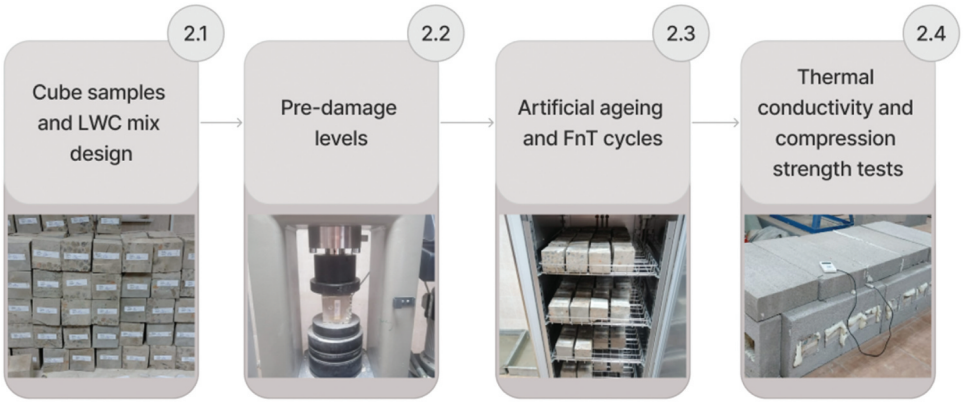

Figure 2. Flowchart of experimental programme.

Figure 3. General view of cubes cut out from LWC wall.

= 250 kg. These mix proportions led to a water–cement ratio of 0.56. Expanded clay aggregate was utilised in this study to replicate LWC which was typically used in the construction of residential buildings in Kazakhstan in the 1950s. The expanded clay aggregates utilised in this study conform to the local standard GOST 9757-90 "Artificial porous gravel, crushed stone, and sand – Specifications" (1990), which recommend the use of fine aggregates with a maximum size of 5 mm, and of coarse aggregates ranging from 5 to 40 mm. Following casting, the LWC wall was cured in water at 18°C for 28 days, after which the 100 mm cubes were cut out from the wall. The cutting was done carefully with a diamond blade to avoid any damage to the LWC cubes.

Initially, 6 cubes were tested to obtain reference results of the original LWC, including the average 28-day compressive strength (f_c) according to EN 12390–3 (BSI 2019), as well as the thermal conductivity (k_c), dry mass (m), and density (ρ_c). The mean results obtained from the 6 cubes were: f_{cm} = 25.9 MPa (standard deviation = 2.25 MPa), thermal conductivity k_c = 0.921 W/mK (determined experimentally as described later in section 2.4), and density ρ_c = 1707 kg/m^3. These figures agree well with results for LWC samples reported previously in the literature e.g. f_c = 14.8–66.8 MPa, k_c = 0.3–1.1 W/mK (BSI 2011), and ρ_c = 1440–1890 kg/m^3 (ESCSI 2007; Kaur et al. 2023).

2.2. Pre-damaged levels

From the 108 cubes left, 90 cubes were subjected to uniaxial compression to pre-damage the samples. The pre-damaged levels (DLs) were defined as a percentage of the 28-day mean compressive strength obtained from the 6 reference cubes (i.e. as a % of f_{cm} = 25.9 MPa) tested according to EN 12390-3. To the best of the authors' knowledge, there are no established standards to define DLs. Previous studies used DLs ranging from 30% to 95% of the mean compressive cube or cylinder strength (e.g. Ferrotto, Fischer, and Niedermeier 2018; Ma et al. 2019; Micelli, Cascardi, and Aiello 2018; Wu et al. 2014). In this study, five DLs were chosen: 40%, 60%, 75%, 85% and 95% of f_{cm}. A 40% DL is deemed to represent the upper (elastic) limit of concrete behaviour, whereas 95% represents damage deemed as concrete "failure". As a result, 18 cubes were tested for each of the DLs mentioned above. The remaining 18 cubes were left intact (DL = 0%) and were therefore considered as undamaged control cubes.

2.3. Artificial ageing and FnT cycles

The 108 undamaged and pre-damaged concrete cubes were subjected to 30, 60, 90, 120, 150 or 180 FnT cycles, following the GOST 10060-2012 (ISC 2018) standard, which is adopted for freeze-thawing studies on concrete in Kazakhstan. Initially, the cubes were immersed in a NaCl solution for 6 h. The solution consisted of 97% tap water and 3% NaCl by mass. Subsequently, the cubes were taken out of the solution, placed into a climate chamber (see Figure 4), and then subjected to freezing (−20°C) for 6 h. After this time, the cubes were heated (+40°C) for 6 h in the same climate chamber to form one full FnT cycle. At every 30 FnT cycles, 18 pre-damaged cubes (i.e. three cubes for each DL) were taken out of the chamber and dried out in an oven for 12 h to subsequently perform the TC (k_c) tests and to determine the RCS ($f_{c,\,res}$) in a cube crusher. In this study, the RCS is defined as the strength resisted by the cubes after experiencing damage, measured as a percentage of its original (undamaged) compressive strength.

2.4. Thermal conductivity tests

To measure the TC of the LWC cubes, a modified version of the hot-guarded plate (HGP) test was adopted. The HGP test is widely used to measure the TC of concrete due to its cost-effectiveness and accurate results (Patel, Patel, and Patel 2016). However, unlike typical HGP tests where samples are sliced out to a maximum thickness of 40 mm, this study determined the TC of LWC using the tested cubes. This was done because slicing out the cubes would have produced additional damage or accidental loss of material in the cubes, as reported in previous tests (Zhang et al. 2015). Additionally, it would have been difficult to perform compressive strength tests (to get the RCS) on very thin samples.

Figure 4. View of typical cubes in climate chamber before first FnT cycle.

An ad-hoc experimental rig was built using aerated "foam" blocks of 625 × 250 × 100 mm, according to the setup shown in Figure 5(a). Five blocks served as a base of the rig (Figure 5(a)), whereas six lateral blocks served as "walls". The lateral blocks had four openings of size 105 × 105 mm each (Figure 5(b)), which in turn hosted the LWC cubes during the tests. Five blocks sealed the top of the rig, as shown in Figure 5(c). The blocks had a TC = 0.13 W/mK and a density $\rho = 800$ kg/m^3, as reported by the local producer. The heating source was positioned in the middle of the rig, as shown in Figure 5(a). To prevent potential heat leakages, the gaps around all cubes and between the blocks were tightly sealed with expansive foam (Figure 5(c)). The ad-hoc rig allowed the transfer of heat only through the cubes hosted in the openings of the foam blocks. Thermocouple sensors were glued using a thermal paste to the internal and external faces of each cube, as shown in Figure 5(d). The thermal paste had a TC = 14.925 W/mK, thus ensuring a maximum heat conduction during the tests. The tests were conducted under standard laboratory conditions, with constant temperature and relative humidity over the testing period.

The cubes were subjected to heat for 6 h using an electric heater placed inside the ad-hoc rig. During this time, the temperatures at the inner ($T_{s,in}$) and outer ($T_{s,out}$) faces of the cubes were measured using the thermocouples shown in Figure 5(d). The readings were then logged into a heat-flow meter. Based on the measured temperatures, the TC value for each cube was calculated using Fourier's equation:

$$-k_c = \frac{Qt}{\Delta TA} \tag{1}$$

where k_c is the TC (in W/mK), Q is the energy transferred through the cube, t is the thickness of the cubes (100 mm), ΔT is the temperature difference between the inner and outer faces of the cube, and A is the area of the cube exposed to the heat source. It should be noted that Equation (1) was used to calculate the results presented and discussed later in Section 3.

After the TC tests, each batch of 18 cubes for different DLs were subjected to compressive tests according to BS EN 12390-3 (BSI 2019) to determine their RCS ($f_{c,res}$).

3. Experimental results and discussion

Table 1 summarises the average TC ($k_{c,avg}$) and RCS ($f_{c,res,avg}$) results from the LWC cubes tested with different DLs and FnT cycles. The table also compares the

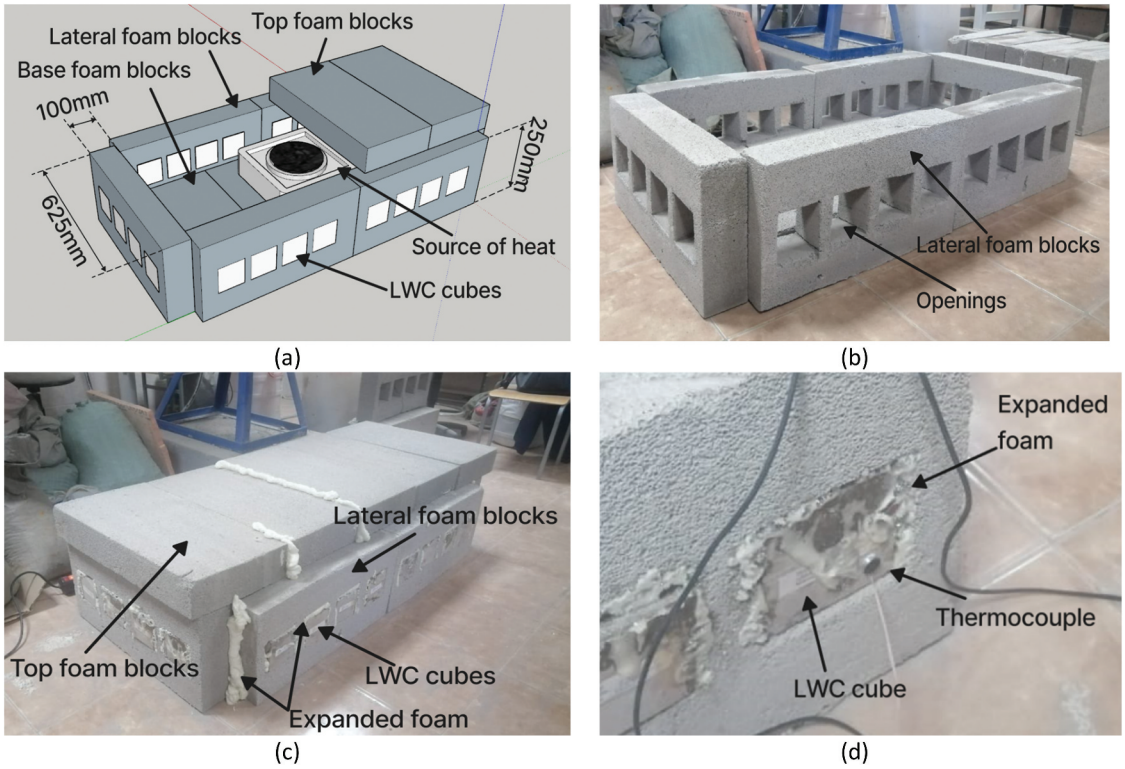

Figure 5. Ad-hoc experimental rig (a) schematic view and dimensions, (b) side view of rig during construction, (c) final view rig during testing, and (d) typical location of thermocouples on a LWC cube.

Table 1. Average $k_{c,avg}$ and $f_{c,res,avg}$ results obtained from tested cubes. Units: $k_{c,avg}$ (W/mK); $f_{c,res,avg}$ (MPa).

FnT		DL 0%	Δ[a] (%)	DL 40%	Δ (%)	DL 60%	Δ (%)	DL 75%	Δ (%)	DL 85%	Δ (%)	DL 95%	Δ (%)
30	$k_{c,avg}$	0.891	−3	0.793	−14	0.748	−19	0.719	−22	0.643	−30	0.518	−43
	$f_{c,res,avg}$	24.8	−4	22.6	−12	21.6	−16	20.9	−19	19.1	−26	20.3	−22
60	$k_{c,avg}$	0.7	−24	0.708	−23	0.712	−23	0.589	−36	0.63	−32	0.499	−46
	$f_{c,res,avg}$	21.8	−16	20.3	−21	18.7	−28	19.7	−24	19.8	−23	14.8	−43
90	$k_{c,avg}$	0.658	−29	0.613	−33	0.608	−34	0.554	−40	0.505	−45	0.496	−46
	$f_{c,res,avg}$	19.7	−24	19.8	−23	18.2	−29	17.6	−32	16.8	−35	15.9	−39
120	$k_{c,avg}$	0.604	−34	0.59	−36	0.536	−42	0.532	−42	0.496	−46	0.457	−50
	$f_{c,res,avg}$	19.4	−25	18.6	−28	18.1	−30	17.4	−33	15.3	−41	14.9	−42
150	$k_{c,avg}$	0.561	−39	0.536	−42	0.511	−45	0.51	−45	0.481	−48	0.479	−48
	$f_{c,res,avg}$	19	−26	18.4	−29	17.1	−34	15.6	−40	13.9	−46	11.4	−56
180	$k_{c,avg}$	0.496	−46	0.488	−47	0.471	−49	0.452	−51	0.451	−51	0.332	−64
	$f_{c,res,avg}$	15.1	−41	18.2	−29	15.5	−40	14.8	−43	10.8	−58	11.3	−56

[a]Δ = percentage changes compared to reference cubes: k_c = 0.921 W/mK; f_c = 25.9 MPa.

difference in results (Δ) over the corresponding results obtained from the first 6 reference cubes (see Section 2.1). Each result in Table 1 is the average of three cubes. The full results for individual cubes are reported in Table A1 of Appendix A. It should be noted that five cubes broke down whilst handling them during the FnT tests, and therefore their results are not reported in Table A1.

The results in Table 1 show that the pre-damage level DL and number of FnT cycles affect the LWC properties. Indeed, LWC cubes with high DL experienced higher reductions (Δ) in TC and RCS as the number of FnT cycles increased. For example, at 150 FnT cycles, the TC of concrete with DL = 0% reduced by 39% compared to the reference results, whereas for concrete with DL = 95% such reduction was 48%. Likewise, the RCS at 150 FnT cycles for DL = 0% reduced by 26% compared to the reference value, whereas for DL = 95% such reduction was 56%. These observations suggest that the thermo-mechanical properties of LWC are affected by both FnT cycles and the pre-damaged levels.

3.1. Comparison of experimental TC and RCS with past studies' results

Figure 6(a) compares the average TC results ($k_{c,avg}$) for different pre-damaged levels (DLs) of the tested LWC cubes vs. results obtained by Perkowski (2008), Delpak, Gailius, and Žukauskas (2002), and Zhang et al. (2015), who only investigated normal concrete specimens (shown as NWC). In Figure 6(a), the TC of each DL was normalised by dividing each TC

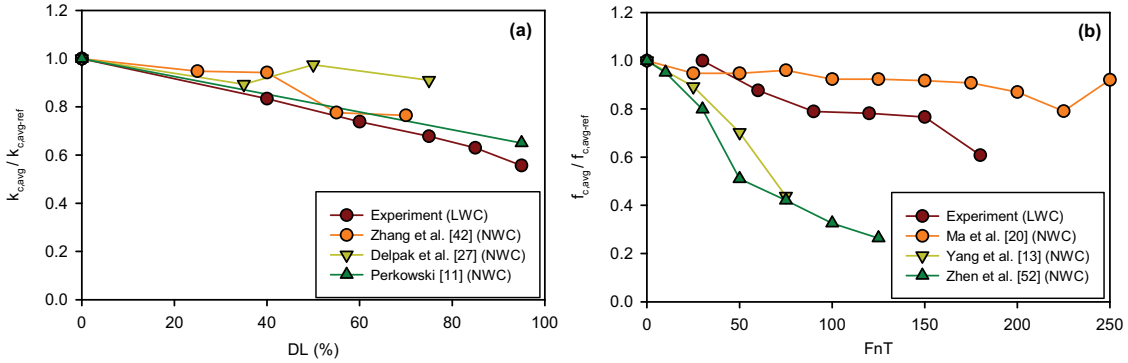

Figure 6. Comparison of the normalised experimental results with past research results, (a) TC vs. DL, and (b) RCS vs. FnT cycles.

datapoint by the initial reference value of TC reported in each of the above studies. The results in Figure 6(a) show that the TC results reported in the abovementioned studies differed from the experimental results obtained from the LWC cubes tested here. Indeed, normal concrete had higher TC (by up to 40%) over the experimental results for LWC, particularly at high damage levels (DLs > 50%). Likewise, Figure 6(b) compares the RCS results ($f_{c,res,avg}$) for different FnT cycles of the tested cubes vs. normal concrete results obtained by Yang et al. (2019), Ma, Zhao, and Yang (2017), and Zheng et al. (2022). In this figure, the results were also normalised over the reference values reported in such studies. It is shown that Yang et al. (2019) and Zhang et al. (2015) reported lower RCS results by up to 36% compared to the LWC cubes tested here. However, Ma, Zhao, and Yang's (2017) results showed higher RCS (up to 50%) compared to the LWC results at 175 FnT. This can be attributed to use of air entrained concrete in Ma et al.'s study, which has a lower deterioration effect compared to normal concrete. The results in Figure 6(a-b) suggest that the TC and RCS changed due to the pre-damaged induced to the cubes and that the TC and RCS results obtained from tests on normal concrete are not fully representative of LWC.

3.2. Thermal conductivity vs. pre-damaged level

Figure 7 compares the average TC ($k_{c,\ avg}$) vs. pre-damaged levels (DLs) of the LWC cubes subjected to different FnT cycles. The results show that the DL significantly influenced the TC of the tested LWC cubes. For instance, at 30 FnT cycles, the TC of cubes with DL = 95% ($k_{c,avg}$ = 0.518 W/mK) was 58% lower than that of cubes at DL = 0% ($k_{c,avg}$ = 0.891 W/mK). The same observation is valid for other FnT cycles, with consistent reductions in TC with increasing DLs. This reduction in TC was also reported in normal concrete specimens tested by Delpak, Gailius, and Žukauskas (2002) and Zhang et al. (2015) at DL = 0% and 95%, with reductions of up to 25% and 16%, respectively.

The results in Figure 7 also indicate that some of the tested cubes experienced an increase in TC at certain FnT cycles (e.g. at 90, 150 and 180 cycles). At a relatively low DL = 40%, this variation can be partly attributed to the natural variability of concrete. However, at DL > 60%, such increase could also be due to the reduction of internal voids in the tested cubes, which in turn results in a denser and more

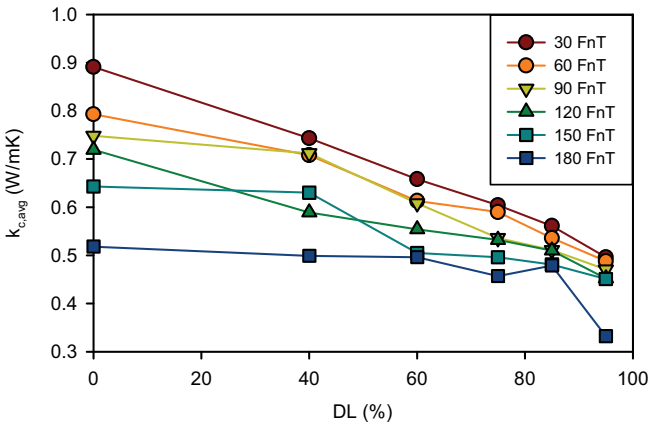

Figure 7. TC vs. DL for different FnT cycles.

compact internal structure. As a result, the cubes with a denser structure showed higher TC compared to the initially intact cubes. However, the increase in TC can also be attributed to other factors such as the change of the experimental conditions (e.g. slight variations of moisture or temperature on the testing day) or to outlier results. It should be noted that Delpak, Gailius, and Žukauskas (2002) and Zhang et al. (2015) also reported an increase in TC with an increase in pre-damaged levels, and therefore the results in Figure 7 are fully consistent with previous experimental findings.

3.3. Reduced compressive strength vs. pre-damaged level

Figure 8 compares the RCS of the LWC cubes vs. pre-damaged levels (DL) for different FnT cycles. The results in Figure 8 show that $f_{c,res,avg}$ reduced consistently as the DL and number of FnT cycles increased. For instance, at DL = 95%, the RCS at 180 FnT cycles ($f_{c,res,avg}$ = 11.3 MPa) was 56% lower than the corresponding value at 30 FnT cycles ($f_{c,res,avg}$ = 20.3 MPa). The results in Figure 8 suggest that the RCS of LWC cubes reduces progressively due to pre-damaged, thus having a similar trend as that observed in Figure 7 for the TC results.

3.4. Thermal conductivity vs. reduced compressive strength

The results from Figures 7 and 8 indicate that both the RCS and TC of the tested LWC cubes reduce with the induced damage, whether this is produced by pre-loading or by the application of FnT cycles. To examine the trends in results, Figure 9 combines the data from both Figures 7 and 8 and compares the average RCS ($f_{c,res,avg}$) vs. TC ($k_{c,avg}$) for different FnT cycles. The results in Figure 9 indicate that, with the exception of a few outliers at 150 and 180 FnT cycles, the relationship between $k_{c,avg}$ and $f_{c,res,avg}$ follows an approximate linear trend regardless of the number of FnT cycles. The outliers can be attributed to the large number of FnT cycles applied to the cubes, which may have led to large variability in results. The results in Figure 9 also show that $f_{c,res,avg}$ and $k_{c,avg}$ consistently decrease as the number of FnT cycles increase, as evidenced by the trendlines included in the figure. However, the slope of the trendlines follows a somewhat similar pattern, which suggests a correlation between $k_{c,avg}$ and $f_{c,res,avg}$. In view of this, the data in Figure 9 (i.e. Table 1) are used in the following section to propose a new practical model to predict the RCS of pre-damaged LWC subjected to FnT cycles.

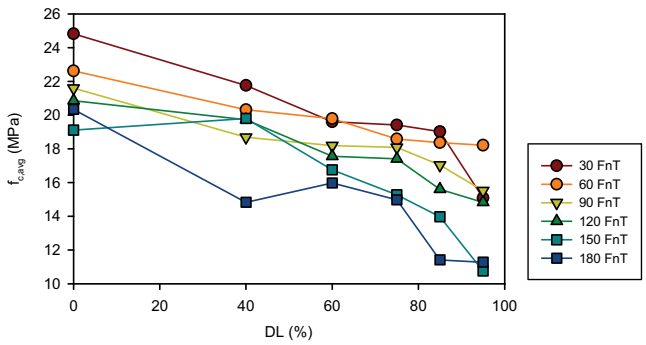

Figure 8. RCS vs DL for different FnT cycles.

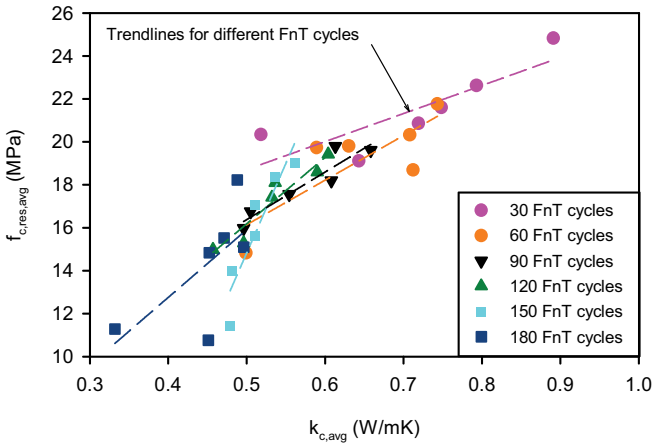

Figure 9. RCS vs. TC for different FnT cycles.

4. A new practical model for RCS of pre-damaged LWC

The proposed model relates the TC and RCS of LWC by adopting i) Maxwell's model for thermal conductivity (Maxwell 1873) by considering LWC as a heterogeneous material according to Equation (2), and ii) a damage coefficient originally proposed by Zhang et al. (2015) for normal concrete subject to damage, according to Equation (3):

$$k_c = k_0\left(\frac{2-2d}{2+d}\right) \tag{2}$$

$$d = 1-\frac{E_c}{E_0} \tag{3}$$

where k_c = TC of damaged concrete, k_0 = TC of undamaged concrete, d = damage coefficient, and E_c = modulus of elasticity of damaged concrete, and E_0 = modulus of elasticity of undamaged concrete.

In this study, it is proposed to calculate the modulus of elasticity (E_c) of LWC using the following formula included in ACI 318 (2007):

$$E_c = 0.043q^{1.5}\sqrt{f'_c} \tag{4}$$

where f'_c = compressive strength of LWC, and q = density of LWC.

By substituting Equation (2), (3) and (4) into Equation (1) and rearranging terms, the following practical model is proposed to predict the RCS ($f_{c,res}$) of LWC based on its TC:

$$f_{c,res} = C_{LWC}\left[\frac{E_c\left(1-\frac{2k_0-2k_c}{k_c+2k_0}\right)}{0.043q^{1.5}}\right]^2 \tag{5}$$

where C_{LWC} = coefficient that considers the relationship between the average RCS ($f_{c,res,avg}$) and TC ($k_{c,avg}$) for different FnT cycles. Based on the data shown in Figure 9 and until more experimental data become available, it is proposed to adopt a value $C_{LWC} = \frac{1}{\sqrt{4.2}}$ in the calculations. As such, C_{LWC} considers the effect of damage onto the $k_{c,avg}$ and $f_{c,res,avg}$ relationship of LWC. It should be noted that Equation (5) is valid for density in the range of 1200 to 1600 kg/m^3. Whilst it is acknowledged that the RCS of pre-damaged LWC can depend on other factors (moisture contents, temperature, strain rate), the main purpose of Equation (5) is to provide a practical formula that can be incorporated into a novel framework recently proposed by the authors (Kargin et al. 2022) that can assess damage of existing LWC buildings using satellite infrared images and AI using cities in Kazakhstan. The proposed model is thus advantageous as it can provide values of RCS ($f_{c,res}$) of LWC using TC as input, which in turn can be easily obtained by doing on-site TC tests for groups of buildings.

To assess the accuracy of the proposed model, Figure 10 compares the experimental results from the LWC cubes and the results predicted by Equation (5). The results indicate that Equation (5) can predict the experimental results presented in this study with sufficient accuracy, apart from some outliers at high DLs (which can be attributed to the very heavy damage applied to the cubes). Table B1 in Appendix B summarises the numerical results plotted in Figure 10, which shows a good fitting as confirmed by a mean Test/Prediction (T/P) ratio and a standard deviation (Std.Dev.) of 1.0 and 0.15, respectively. Therefore, it can be concluded that the proposed model (i.e. Equation (5)) predicts reasonably well the RCS of LWC.

5. Evaluation of proposed model

To evaluate the effectiveness of the proposed model at predicting the RCS of LWC, concrete core cylinders were cored from real LWC wall panels of an existing building located in Karaganda city, Kazakhstan (see Figure 11). Karaganda experiences average temperatures of −20°C in winter and + 25°C in the summer, with an average relative humidity of 70-80%. The selected building is representative of typical buildings

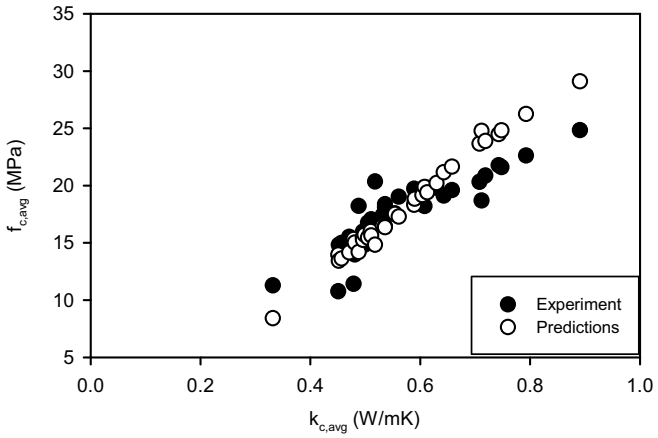

Figure 10. Comparison between experimental and results precited by the model proposed in Equation (5).

Figure 11. Existing PC LWC building in Karaganda city, Kazakhstan.

built in the 1950s with LWC panels. The building has been inhabited since 1993 due to a high risk of collapse caused by the deterioration and damage of the LWC wall panels. All windows and doors were removed in 1993 and therefore, when the cored cylinders were extracted, the LWC wall panels had been exposed to FnT cycles (on both faces of the wall) for 30 years due to the harsh continental climate in the region. It should be noted that whilst the LWC wall was not exposed to the same FnT cycles as the cubes (reported in section 2.3), a close visual inspection of the LWC revealed that damage due to FnT had indeed occurred over time. Moreover, cylinders were cored from the LWC wall due to the difficulties of extracting cubes on-site.

Figure 12(a) shows the five cored cylinders, which had a diameter ⌀100 and length 380 mm. One of the cylinders had a reinforcing bar in the middle portion and thus it was ignored in the validation. The other four cylinders were tested in the laboratory to obtain their TC by applying heat using a heat source at the bottom of the cylinders, as shown in Figure 12(b). The TC readings were then taken using a heat-flow meter. All measurements were made by applying temperature measurement probes to the heated and unheated ends of the cylinders. To prevent heat loss between the probe and the sample surface, a thermal paste with a thermal conductivity = 14.925 W/mK was used. The compressive strength of the four LWC cylinders was subsequently obtained from shorter ⌀100 × 200 mm samples ($f_{cm,avg}$ = 13.47 MPa; Std.Dev. = 1.42 MPa) according to BS EN 12390-3 (BSI 2019), as shown in Figure 12(c).

To compare the on-site (cored cylinders) results and the cube results for LWC, it was assumed that the cylinder strength was 90% of the cube strength as per EN 206 (CEN 2021). Table 2 compares the results from cored cylinders and the predictions given by the proposed model, including the corresponding mean T/P ratio and Std.Dev. The results in Table 2 indicate that the proposed model predicts well the RCS of the cored cylinders with a mean T/P = 1.13 and Std.Dev. = 0.26. However, additional cored samples from more buildings are required for a more comprehensive validation of the proposed model.

The results in this article indicate that the new proposed model (i.e. Equation (5)) is suitable to calculate the RCS of pre-damaged LWC cubes subjected to freezing-thawing cycles. The proposed model only

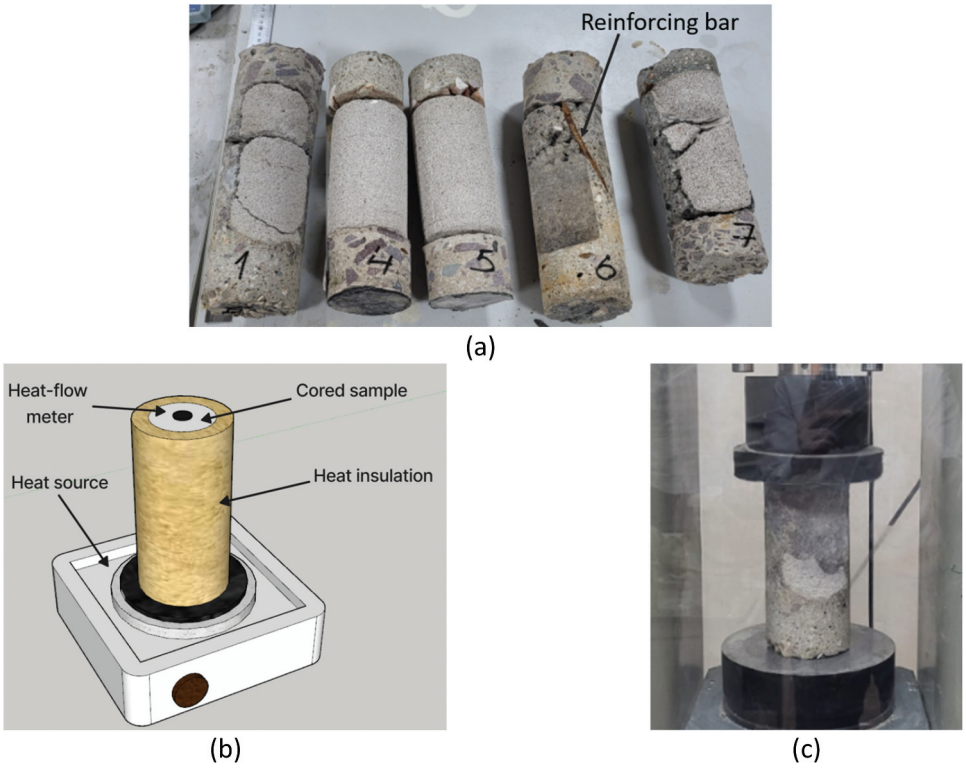

Figure 12. Cored samples (a) cylinders of LWC from actual building, (b) thermal conductivity test, and (c) compressive strength test.

Table 2. Comparison between cored cubes results and proposed model.

Cored cylinders (Test)		Proposed model (Predictions Equation (5))		
k_c	$f_{c,res}$	k_c	$f_{c,res}$	T/P
(W/mK)	(MPa)	(W/mK)	(MPa)	
0.453	12.6	0.332	8.4	1.50
0.472	13.5	0.451	14.0	0.96
0.473	12.3	0.452	13.4	0.92
0.502	15.5	0.457	13.6	1.14
			Mean	1.13
			Std.Dev.	0.26

depends on the thermal conductivity (TC) of the LWC because the experimental results showed that the relationship between the TC and RCS follows an approximate linear trend regardless of the number of FnT cycles.

It should be noted that the experimental results in this study were obtained from LWC cubes produced with expanded clay as coarse aggregate and local sand from central Kazakhstan. Therefore, the proposed model and experimental results require validation with different concrete mix designs, including the use of various coarse aggregates (e.g. pumice stone (Nimat, Mohammed, and Mohammed 2023)) or recycled concrete (Neupane et al. 2023), as well as different types of LWC, including expanded polystyrene (EPS) concrete (Ahmed and Mohammed 2024). Additionally, samples with different dimensions and geometries should be tested to examine potential size effects, which can affect the magnitude of the RCS measured in tests. Further tests are also necessary to determine if the proposed value $C_{LWC}=\frac{1}{\sqrt{4.2}}$ is valid for other pre-damage levels and different number of FnT cycles to those adopted in this article. Whilst the data presented in this article were obtained under a standard laboratory setting (with controlled temperature and relative humidity), variations in laboratory conditions can affect the TC measurements. As a result, additional results from other laboratories and testing environments are needed to evaluate the accuracy of the new RCS model. Additionally, the proposed model requires further validation with more cored samples extracted from actual buildings. It should also be noted that the level of pre-damaged and number FnT cycles can affect the porosity and permeability of LWC. Such concrete properties were not directly measured in this study, and therefore this is a matter of future research. Despite the above limitations, the proposed RCS prediction model is deemed as sufficiently accurate to calculate the RCS of LWC buildings, thus being suitable to assess the structural conditions of buildings located in continental climates.

6. Summary and conclusions

This article proposes a new practical thermal-based model to calculate the reduced compressive strength (RCS) of pre-damaged lightweight concrete (LWC) subjected to freezing-thawing (FnT) cycles. The new model adopts Maxwell's equation for thermal conductivity (TC) and a damage coefficient proposed by Zhang et al. (2015). To achieve this, 108 concrete cubes (size 100 mm) were subjected to different pre-damaged levels (DL = 0%, 40%, 60%, 75%, 85% or 95%) and various FnT cycles (30, 60, 90, 120, 150 or 180 cycles). Based on the experimental results, the new model is calibrated and subsequently evaluated against test results from cylinders cored from actual LWC wall panels of an existing building in Kazakhstan, which has been exposed to FnT cycles for 30 years. Based on the results presented in this article, the following conclusions can be drawn:

6.1. Main findings

(1) The TC of the tested cubes consistently reduced as the level of pre-damage and number of FnT cycles increased. For example, at 30 FnT cycles, the TC of severely damaged cubes with DL = 95% (0.518 W/mK) was 58% lower than that of cubes at DL = 0% (0.891 W/mK). The RCS also consistently dropped with the applied FnT cycles. For instance, at DL = 95%, the RCS at 180 FnT cycles (11.3 MPa) was 56% lower than the corresponding value at 30 FnT cycles (20.3 MPa). However, for the LWC cubes tested in this study, the experimental TC and RCS followed an approximately linear trend regardless of the number of FnT cycles applied during the tests.

(2) The new proposed model (i.e. Equation 5) predicted well the RCS of the tested LWC cubes, with a mean Test/Prediction (T/P) ratio of 1.0 and a Std.Dev. of 0.15. This was achieved by adopting a value $C_{LWC}=\frac{1}{\sqrt{4.2}}$ in the calculations, where C_{LWC} considers the effect of damage onto the TC ($k_{c,avg}$) and RCS ($f_{c,res,avg}$) relationship of LWC.

(3) The effectiveness of the new proposed model was evaluated against results from four LWC cylinders cored from an actual building in Karaganda (Kazakhstan) that has been exposed to FnT cycles for 30 years. The proposed model predicted well the RCS of the cored cylinders, giving a mean T/P ratio of 1.13 with a Std.Dev. of 0.26. This suggests that the proposed model is

suitable for calculating the RCS of pre-damaged LWC subjected to freezing-thawing cycles.

6.2. Research limitations and further research needs

The results reported in this article should be considered in the light of some limitations. The experimental results obtained from LWC cubes produced with expanded clay (coarse aggregate) and local sand from central Kazakhstan. Therefore, the proposed model and experimental results require validation with different concrete mix designs, including the use of various coarse aggregates (e.g. pumice stone and other natural stones), as well as different types of LWC, including EPS concrete. Additionally, samples with different dimensions and geometries should be tested to examine potential size effects, which can affect the magnitude of the RCS measured in tests. Moreover, additional data with different FnT cycles and different levels of pre-damage are necessary to verify the accuracy of the proposed model. Further tests are also necessary to determine if the proposed value $C_{LWC}=\frac{1}{\sqrt{4.2}}$ is valid for other pre-damage levels and different number of FnT cycles to those adopted in this article. Whilst the data presented in this article were obtained under a standard laboratory setting (with controlled temperature and relative humidity), variations in laboratory conditions can affect the TC measurements. As a result, additional results from other laboratories and testing environments are needed to evaluate the accuracy of the new RCS model. Additionally, the proposed model requires further validation with more cored samples extracted from actual buildings. It should be also noted that the level of pre-damage and number FnT cycles can affect the porosity and permeability of LWC. Such concrete properties were not directly measured in this study, and therefore this is a matter of future research.

Acknowledgements

M.K. gratefully acknowledges the financial support provided by BOLASHAK Kazakhstan to pursue his PhD studies. S.N.R., R. G. and I.L. thankfully acknowledge the financial support provided by the Monash Warwick Alliance Activation Fund 2024. Part of this project was conducted within the Reinventing Project, 'Blue Ocean for Enhancing Thai Universities into International Education' under the Ministry of Higher Education, Science, Research and Innovation of Thailand.

Disclosure statement

No potential conflict of interest was reported by the author(s).

Data availability statement

The data that led to the findings of this article can be obtained from the first author (M.K.) upon reasonable request. However, restrictions may apply as some data were used under explicit permission from third parties located in other countries to where the main research was conducted.

References

ACI Committee 213. 2014. *Guide for Structural Lightweight Aggregate Concrete*. Farmington Hills, VA: American Concrete Institute.

ACI Committee 318. 2007. *ACI 318 - Building Code Requirements for Structural Concrete*. Farmington Hills, VA: American Concrete Institute.

Ahmed, F. R., and A. S. Mohammed. 2024. "Chlorine Salt Influence on Durability and Strength of Additive-Free EPS Lightweight Concrete." *Innovative Infrastructure Solutions* 9 (4). https://doi.org/10.1007/s41062-024-01412-w.

Alengaram, U. J., B. A. Al Muhit, M. Z. Bin Jumaat, and M. L. Y. Jing. 2013. "A Comparison of the Thermal Conductivity of Oil Palm Shell Foamed Concrete with Conventional Materials." *Materials & Design* 51:522–529. https://doi.org/10.1016/j.matdes.2013.04.078.

Antunes Almeida da Silva, A. D. 2015. "Thermal Insulation Characteristics of Structural Lightweight and Normal Weight Concretes Produced with Different Types of Aggregates." *Engineering, Materials Science* 2003:1–12. https://api.semanticscholar.org/CorpusID:195062769.

Asadi, I., P. Shafigh, Z. F. Bin Abu Hassan, and N. B. Mahyuddin. 2018. "Thermal Conductivity of Concrete – A Review." *Journal of Building Engineering* 20:81–93. https://doi.org/10.1016/j.jobe.2018.07.002.

Bamforth, P., D. Chisholm, J. Gibbs, Harrison, T. 2008. *Properties of concrete for use in Eurocode 2*. 1st ed., 59. Surrey: The Concrete Centre.

Bao, J., S. Xue, P. Zhang, Z. Dai, and Y. Cui. 2021. "Coupled Effects of Sustained Compressive Loading and Freeze–Thaw Cycles on Water Penetration into Concrete." *Structural Concrete* 22 (S1): E944–E954. https://doi.org/10.1002/suco.201900200.

Bindiganavile, V., F. Batool, and N. Suresh. 2012. "Effect of Fly Ash on Thermal Properties of Cement Based Foams Evaluated by Transient Plane Heat Source." *Indian Concrete Journal* 86 (11): 7–14.

BSI. 2011. *BS EN 1992-1-1 Eurocode 2 - Design of concrete structures - Part 1-1: General rules*. London: British Standards Institution.

BSI. 2019. *BS EN 12390-3:2019 - Testing Hardened Concrete - Part 3: Compressive Strength of Test Specimens*. London: British Standards Institution.

Campbell-Allen, D., C. P. Thorne, N. G. Zoldners, V. M. Malhotra, and M. Levitt. 1964. "The Thermal Conductivity of Concrete." *Magazine of Concrete Research* 16 (49): 233–234. https://doi.org/10.1680/macr.1964.16.49.233.

Cao, D., J. Liu, Y. Zhou, W. Ge, X. Zhang, and A. Babafemi. 2021. "Experimental Study on the Effect of Freeze-Thaw Cycles on Axial Tension and Compression Performance of Concrete After Complete Carbonization." *Advanced Civil Enginering* 2021 (1). https://doi.org/10.1155/2021/8111436.

CEN. 2021. *EN 206:2013: Concrete. Specification, performance, production and conformity*. Brussels: European Committee for Standardisation.

Choktaweekarn, P., W. Saengsoy, and S. Tangtermsirikul. 2009. "A Model for Predicting Thermal Conductivity of Concrete." *Magazine of Concrete Research* 61 (4): 271–280. https://doi.org/10.1680/macr.2008.00049.

Colombo, I. G., M. Colombo, and M. Di Prisco. 2015. "Tensile Behavior of Textile Reinforced Concrete Subjected to Freezing-Thawing Cycles in Un-Cracked and Cracked Regimes." *Journal of Cement and Concrete Research* 73:169–183. https://doi.org/10.1016/j.cemconres.2015.03.001.

Delpak, R., A. Gailius, and D. Žukauskas. 2002. "Determination of Thermal-Mechanical Properties of Concrete." *Journal of Civil Engineering and Management* 8 (2): 121–124. https://doi.org/10.1080/13923730.2002.10531263.

ESCSI. 2007. *Properties of Walls Using Lightweight Concrete and Lightweight Concrete Masonry Units*, 11.2–6. 1st ed. Salt Lake City: Expanded Shale, Clay & Slate Institute (ESCSI).

Ferrotto, M. F., O. Fischer, and R. Niedermeier. 2018. "Experimental Investigation on the Compressive Behavior of Short-Term Preloaded Carbon Fiber Reinforced Polymer-Confined Concrete Columns." *Structural Concrete* 19 (4): 988–1001. https://doi.org/10.1002/suco.201700072.

Gao, Y., X. Ren, J. Zhang, L. Zhong, S. Yu, X. Yang, and W. Zhang. 2020. "Proposed Constitutive Law of Uniaxial Compression for Concrete Under Deterioration Effects." *Materials (Basel)* 13 (9): 2048. https://doi.org/10.3390/MA13092048.

Hrabovszky-Horváth, S., and Z. Szalay. 2014. "Environmental Assessment of a Precast Concrete Building Stock in a Time Perspective." *Environmental Engineering and Management Journal* 13 (11): 2797–2804. https://doi.org/10.30638/eemj.2014.312.

Huang, H., R. Garcia, S. S. Huang, M. Guadagnini, and K. Pilakoutas. 2019. "A Practical Creep Model for Concrete Elements Under Eccentric Compression." *Materials and Structures* 52 (6): 1–18. https://doi.org/10.1617/s11527-019-1432-z.

ISC. 2018. *GOST: 10060-2012, Concretes, Methods for Determination of Frost-Resistance*. Moscow: Interstate Council for Standardization, Metrology and Certification.

Karagöl, F., Y. Yegin, R. Polat, A. Benli, and R. Demirboğa. 2018. "The Influence of Lightweight Aggregate, Freezing–Thawing Procedure and Air Entraining Agent on Freezing–Thawing Damage." *Structural Concrete* 19 (5): 1328–1340. https://doi.org/10.1002/suco.201700133.

Kargin, M., R. Lukpanov, A. Serenkov, Y. Shaymagambetov, J. Kargin, R. Garcia, and I. Laory. 2022. "An Innovative Structural Health Assessment Tool for Existing Precast Concrete Buildings Using Deep Learning Methods and Thermal Infrared Satellite Imagery." *Journal of Civil Structural Health Monitoring* 13 (123456789): 561–578. https://doi.org/10.1007/s13349-022-00655-4.

Kaur, N., C. C. Lee, A. Mostafavi, and A. Mahdavi-Amiri. 2023. "Large-Scale Building Damage Assessment Using a Novel Hierarchical Transformer Architecture on Satellite Images." *Computers in Civil and Infrastructure Engineering* 38 (15): 2072–2091. https://doi.org/10.1111/mice.12981.

Kosior-Kazberuk, M. 2013. "Variations in Fracture Energy of Concrete Subjected to Cyclic Freezing and Thawing." *Archives of Civil and Mechanical Engineering* 13 (2): 254–259. https://doi.org/10.1016/j.acme.2013.01.002.

Liu, D., C. Wang, J. Gonzalez-Libreros, T. Guo, J. Cao, Y. Tu, L. Elfgren, and G. Sas. 2023. "A Review of Concrete Properties Under the Combined Effect of Fatigue and Corrosion from a Material Perspective." *Construction and Building Materials* 369 (January): 130489. https://doi.org/10.1016/j.conbuildmat.2023.130489.

Lu, X., F. Tong, G. Liu, and J. Guan. 2021. "Model for Predicting the Thermal Conductivity of Concrete." *International Journal of Thermophysics* 42 (3): 1–20. https://doi.org/10.1007/s10765-020-02786-6.

Ma, C.-K., R. Garcia, S. C. S. Yung, A. Z. Awang, W. Omar, and K. Pilakoutas. 2019. "Strengthening of Pre-Damaged Concrete Cylinders Using Post-Tensioned Steel Straps." *Proceedings of the Institution of Civil Engineers - Structures and Buildings* 172 (10): 703–711. https://doi.org/10.1680/jstbu.18.00031.

Ma, Z., T. Zhao, and J. Yang. 2017. "Fracture Behavior of Concrete Exposed to the Freeze-Thaw Environment." *Journal of Materials in Civil Engineering* 29 (8). https://doi.org/10.1061/(asce)mt.1943-5533.0001901.

Maxwell, J. C. 1873. *A Treatise on Electricisty and Magnetism*. Oxford: Clarendon Press Series.

Micelli, F., A. Cascardi, and M. A. Aiello. 2018. "A Study on FRP-Confined Concrete in Presence of Different Preload Levels." 9th International Conference on Fibre-Reinforced Polymer Composites for Civil Engineering (CICE), 493–499. Paris, France.

Misri, Z., M. H. W. Ibrahim, A. S. M. A. Awal, M. S. M. Desa, and N. S. Ghadzali. 2018. "Review on Factors Influencing Thermal Conductivity of Concrete Incorporating Various Type of Waste Materials." *IOP Conference Series Earth and Environmental Science* 140 (1): 7–14. https://doi.org/10.1088/1755-1315/140/1/012141.

Neupane, R. P., T. Imjai, N. Makul, R. Garcia, B. Kim, and S. Chaudhary. 2023. "Use of Recycled Aggregate Concrete in Structural Members: A Review Focused on Southeast Asia." *Journal of Asian Architecture and Building Engineering*: 1–24. https://doi.org/10.1080/13467581.2023.2270029.

Nimat, A. J., A. A. Mohammed, and A. S. Mohammed. 2023. "Evaluation of Fracture Mechanics Parameters of Light-Weight Concrete by Implementing Natural Pumice Stone as Coarse Aggregate." *Sulaimania Journal for Engineering Sciences* 9 (3): 61–74. https://doi.org/10.17656/sjes.10162.

Othuman, M. A., and Y. C. Wang. 2011. "Elevated-Temperature Thermal Properties of Lightweight Foamed Concrete." *Construction and Building Materials* 25 (2): 705–716. https://doi.org/10.1016/j.conbuildmat.2010.07.016.

Pan, P., S. Wu, X. Hu, P. Wang, and Q. Liu. 2017. "Effect of Freezing-Thawing and Ageing on Thermal Characteristics and Mechanical Properties of Conductive Asphalt Concrete." *Construction and Building Materials* 140 (June): 239–247. https://doi.org/10.1016/j.conbuildmat.2017.02.135.

Patel, R., C. Patel, and P. Patel. 2016. "A Review Paper on Measure Thermal Conductivity." *Journal of Emerging Technologies and Innovative Research* 3 (2): 51–53.

Perkowski, Z. 2008. "Change of Thermal Conductivity of Concrete Caused by Brittle Damage Evolution." *Bauphysik* 30 (6): 434–437. https://doi.org/10.1002/bapi.200810057.

Real, S., M. G. Gomes, A. Moret Rodrigues, and J. A. Bogas. 2016. "Contribution of Structural Lightweight Aggregate Concrete to the Reduction of Thermal Bridging Effect in Buildings." *Construction and Building Materials* 121:460–470. https://doi.org/10.1016/j.conbuildmat.2016.06.018.

Sáez Del Bosque, I. F., P. Van den Heede, N. De Belie, M. I. S. de Rojas, and C. Medina. 2020. "Freeze-Thaw Resistance of Concrete Containing Mixed Aggregate and Construction and Demolition Waste-Additioned Cement in Water and de-Icing Salts." *Construction and Building Materials* 259:119772. https://doi.org/10.1016/j.conbuildmat.2020.119772.

Shang, H., Y. Song, and J. Ou. 2009. "Behavior of Air-Entrained Concrete After Freeze-Thaw Cycles." *Acta Mechanica Solida Sinica* 22 (3): 261–266. https://doi.org/10.1016/S0894-9166(09)60273-1.

Shang, H. S., and Y. P. Song. 2006. "Experimental Study of Strength and Deformation of Plain Concrete Under Biaxial Compression After Freezing and Thawing Cycles." *Journal of Cement and Concrete Research* 36 (10): 1857–1864. https://doi.org/10.1016/j.cemconres.2006.05.018.

Sharikov, B. 2017. "At Least Nine Dead in Kazakhstan Apartment Building Collapse - World - TASS." *TASS, Moscow*. Jan 02.

Shen, L., Q. Ren, L. Zhang, Y. Han, and G. Cusatis. 2017. "Experimental and Numerical Study of Effective Thermal Conductivity of Cracked Concrete." *Construction and Building Materials* 153:55–68. https://doi.org/10.1016/j.conbuildmat.2017.07.038.

SN RK. 1990. GOST 9757-90: Artificial Porous Gravel, Crushed Stone and Sand." *Specifications*. https://online.zakon.kz/Document/?doc_id=30039244&pos=9;-59#pos=9;-59.

Statistics. 2020. "Тұрғын үй қоры туралы О жилищном фонде О жилищном фонде Статистикалық жинақ." *Taraz, Committee of the Ministry of National Economy of the Republic of Kazakhstan*.

Talebi, H. R., B. A. Kayan, I. Asadi, and Z. F. B. A. Hassan. 2020. "Investigation of Thermal Properties of Normal Weight Concrete for Different Strength Classes." *Journal of Environmental Treatment Techniques* 8 (3): 908–914.

Wang, H., Y. Zhou, and J. Yu Shen. 2023. "Experimental Study of Dynamic Biaxial Compressive Properties of Full Grade Aggregate Concrete After Freeze Thaw Cycles." *Cold Regions Science & Technology* 205 (August 2020): 103710. https://doi.org/10.1016/j.coldregions.2022.103710.

Wang, J., J. K. Carson, M. F. North, and D. J. Cleland. 2006. "A New Approach to Modelling the Effective Thermal Conductivity of Heterogeneous Materials." *International Journal of Heat and Mass Transfer* 49 (17–18): 3075–3083. https://doi.org/10.1016/j.ijheatmasstransfer.2006.02.007.

Wardeh, G., M. A. S. Mohamed, and E. Ghorbel. 2011. "Analysis of Concrete Internal Deterioration Due to Frost Action." *Journal of Building Physics* 35 (1): 54–82. https://doi.org/10.1177/1744259110370854.

Woo, B. H., D. H. Yoo, S. S. Kim, J. B. Lee, J. S. Ryou, and H. G. Kim. 2021. "Effects of Thermal Conductive Materials on the Freeze-Thaw Resistance of Concrete." *Materials (Basel)* 14 (15): 4063. https://doi.org/10.3390/ma14154063.

Wu, Y.-F., Y. Yun, Y. Wei, and Y. Zhou. 2014. "Effect of Predamage on the Stress-Strain Relationship of Confined Concrete Under Monotonic Loading." *Journal of Structural Engineering* 140 (12): 1–18. https://doi.org/10.1061/(asce)st.1943-541x.0001015.

Xu, Y., L. Jiang, J. Liu, Y. Zhang, J. Xu, and G. He. 2016. "Experimental Study and Modeling on Effective Thermal Conductivity of EPS Lightweight Concrete." *Journal of Thermal Science and Technology* 11 (2): JTST0023–JTST0023. https://doi.org/10.1299/jtst.2016jtst0023.

Yang, X., G. Wang, S. Gao, M. Song, and A. Wang. 2019. "Equation for the Degradation of Uniaxial Compression Stress of Concrete Due to Freeze-Thaw Damage." *Advances in Materials Science and Engineering* 2019:1–8. https://doi.org/10.1155/2019/8603065.

Zhang, K., J. Zhou, and Z. Yin. 2021. "Experimental Study on Mechanical Properties and Pore Structure Deterioration of Concrete Under Freeze–Thaw Cycles." *Materials (Basel)* 14 (21): 6568. https://doi.org/10.3390/ma14216568.

Zhang, W., H. Min, X. Gu, Y. Xi, and Y. Xing. 2015. "Mesoscale Model for Thermal Conductivity of Concrete." *Construction and Building Materials* 98:8–16. https://doi.org/10.1016/j.conbuildmat.2015.08.106.

Zheng, X., Y. Wang, S. Zhang, F. Xu, X. Zhu, X. Jiang, L. Zhou, et al. 2022. "Research Progress of the Thermophysical and Mechanical Properties of Concrete Subjected to Freeze-Thaw Cycles." *Construction and Building Materials* 330 (March): 127254. https://doi.org/10.1016/j.conbuildmat.2022.127254.

Appendix A. Experimental results of tested cubes

Table A1. Experimental results of tested cubes. Units: k_c (W/mK); $f_{c,res}$ (MPa).

		DL = 0%		DL = 40%		DL = 60%		DL = 75%		DL = 85%		DL = 95%	
FnT cycles		Cube	Avg.	Cube	Avg.	Cube	Avg.	Cube	Avg.	Cube	Avg.	Cube	Avg.
0 (6 reference cubes)	k_c	0.987	0.921	–	–	–	–	–	–	–	–	–	–
		1.08		–		–		–		–		–	
		0.885		–		–		–		–		–	
		0.881		–		–		–		–		–	
		0.705		–		–		–		–		–	
		0.987		–		–		–		–		–	
	$f_{c,res}$	28.0	25.8	–	–	–	–	–	–	–	–	–	–
		24.9		–		–		–		–		–	
		23.6		–		–		–		–		–	
		27.9		–		–		–		–		–	
		25.5		–		–		–		–		–	
		25.1		–		–		–		–		–	
30	k_c	0.865		0.612		0.772		0.708		0.659		0.525	
		0.917	0.891	1.042	0.793	CR	0.748	0.615	0.719	0.983	0.643	0.511	0.518
		CR*		0.726		0.724		0.833		0.287		CR	
	$f_{c,res}$	23.2		26.6		21.4		22.2		19.8		23.8	
		26.4	24.8	28.0	22.6	CR	21.6	30.4	20.9	16.7	19.1	16.8	20.3
		CR*		13.2		21.8		10.1		20.8		CR	
60	k_c	0.838		1.123		0.790		0.574		0.654		0.506	
		0.644	0.706	0.753	0.708	0.716	0.712	0.632	0.589	0.642	0.630	CR	0.499
		0.636		0.248		0.630		0.561		0.594		0.492	
	$f_{c,res}$	22.7		13.9		12.4		29.8		22.4		16.5	
		19.7	21.8	18.6	20.3	18.0	18.7	21.8	19.7	17.4	19.8	CR	14.8
		23.0		28.4		25.6		16.2		19.5		13.1	
90	k_c	0.862		0.434		0.575		0.536		0.487		0.478	
		0.650	0.658	1.027	0.613	0.655	0.608	0.566	0.554	0.498	0.505	0.502	0.496
		0.461		0.377		0.594		0.560		0.530		0.508	
	$f_{c,res}$	12.7		20.6		20.1		11.8		18.7		11.7	
		33.6	19.7	13.5	19.8	18.2	18.2	23.3	17.6	15.8	16.8	16.0	15.9
		13.1		25.4		16.3		17.6		15.78		20.1	
120	k_c	0.591		0.570		0.518		0.514		0.478		CR	
		0.592	0.604	0.610	0.590	0.543	0.536	0.538	0.532	0.502	0.496	0.446	0.457
		0.629		0.590		0.547		0.544		0.508		0.468	
	$f_{c,res}$	31.5		19.9		19.9		17.8		15.6		CR	
		12.2	19.4	19.6	18.6	16.5	18.1	17.4	17.4	11.6	15.3	11.2	14.9
		14.6		16.2		17.9		17.0		18.7		18.6	
150	k_c	0.543		0.512		0.504		0.521		0.487		0.465	
		0.569	0.561	0.542	0.536	0.519	0.511	0.494	0.510	0.521	0.481	0.495	0.479
		0.571		0.554		0.510		0.515		0.435		0.477	
	$f_{c,res}$	24.3		21.8		17.8		16.1		11.8		12.4	
		22.8	19.0	15.3	18.4	19.8	17.1	15.6	15.6	19.5	13.9	10.7	11.4
		9.9		18.1		13.7		15.1		10.7		11.1	
180	k_c	0.483		0.498		0.483		0.446		0.438		0.318	
		0.509	0.496	0.470	0.488	0.456	0.471	0.470	0.452	0.470	0.451	0.347	0.332
		0.496		0.496		0.474		0.440		0.445		0.331	
	$f_{c,res}$	15.9		16.3		12.6		13.8		7.3		12.4	
		12.9	15.1	20.3	18.2	15.5	15.5	13.9	14.8	15.3	10.8	11.4	11.3
		16.6		18.1		18.4		16.8		9.7		10.1	

CR* - broken sample.

Appendix B.

Table B1. Comparison between experimental results and RCS predicted by Eq. (5). Results are the average of three cubes.

Cubes ID	TC Test	RCS Test	RCS Predicted Eq. (5)	T/P
	$k_{c,\ avg,\ exp}$ (W/mK)	$f_{d,\ avg,\ exp}$ (MPa)	$f_{d,\ pred}$ (MPa)	
1 14 17	0.332	11.3	8.4	1.34
32 51 58	0.451	10.8	14.0	0.77
73 46 90	0.452	14.8	13.4	1.10
118 6 62	0.457	15.0	13.6	1.10
101 49 80	0.471	15.5	14.2	1.10
83 78 81	0.479	11.4	15.3	0.75
144 12 31	0.481	14.0	15.0	0.93
130 22 64	0.488	18.2	14.2	1.28
91 69 77	0.496	15.1	15.5	0.97
114 86 110	0.496	15.3	15.4	0.99
34 63 106	0.496	16.0	15.2	1.05
135 99 107	0.499	14.8	15.7	0.95
112 20 40	0.505	16.8	15.4	1.09
48 10 38	0.51	15.6	16.0	0.97
141 11 74	0.511	17.0	15.6	1.09
75 84 95	0.518	20.3	14.8	1.37
105 5 57	0.532	17.4	16.5	1.05
122 79 126	0.536	18.1	16.5	1.10
142 18 96	0.536	18.4	16.4	1.12
109 35 145	0.554	17.6	17.5	1.00
108 75 100	0.561	19.0	17.3	1.10
140 45 47	0.589	19.7	18.3	1.08
82 85 125 132	0.59	18.6	18.8	0.99

(*Continued*)

Table B1. (Continued).

Cubes ID	TC Test	RCS Test	RCS Predicted Eq. (5)	T/P
71 119	0.604	19.4	19.2	1.01
124 116 117	0.608	18.2	19.9	0.92
133 7 72	0.613	19.8	19.4	1.02
93 89 129	0.630	19.8	20.2	0.98
134 37 50	0.643	19.1	21.2	0.90
137 15 56	0.658	19.6	21.6	0.91
59 36 66	0.708	20.3	23.7	0.86
136 4 21	0.712	18.7	24.8	0.76
139 102 123	0.719	20.9	23.9	0.87
127 94 115	0.743	21.8	24.5	0.89
121 111 128	0.748	21.6	24.8	0.87
138 39 98	0.793	22.6	26.2	0.86
103 87 104	0.891	24.8	29.1	0.85
			Mean	**1.00**
			Std.Dev.	**0.15**